

# ULTRASOUND IMAGE MODELLING AND RESOLUTION ENHANCEMENT



Ákos Makra

*Theses of the Ph.D. Dissertation*

Supervisor: Dr. Miklós Gyöngy

Pázmány Péter Catholic University  
Faculty of Information Technology and Bionics  
Tamás Roska Doctoral School of Sciences and  
Technology

Budapest, 2020



# Introduction

Diagnostic ultrasound has been in use for 60 years now and it has become one of the most popular medical imaging methods nowadays. Diagnostic ultrasound imaging commonly utilizes frequencies in the range of 3–20 MHz. The use of higher frequencies limits the depth of penetration, however it also increases resolution.

As of late, ultrasound (US) has been actively used not only for medical diagnostic purposes [1–3], but also for high-intensity focal beam surgery to produce precise and selective damage to tissues [4–6], biometric recognition [7], non-destructive testing [8–18], and has many applications in the food industry [19–22] among others. Its wide range of applications stems from its numerous advantages such as cost-effectiveness, portability, and using non-ionizing radiation compared to many other procedures such as X-ray, CT or PET, all of which are using potentially harmful radiation. On the other hand, the interpretation of US images is still quite a subjective task despite the numerous quantitative US studies [23–32].

The connection between the fine microscopic structure of tissues and the resulting ultrasound image is at present not fully understood, which further motivates the development and the importance of validating image formation models.

# Challenges in ultrasound image resolution enhancement

Imaging modalities of any kind have a theoretical limit on their feasible resolution. The objective of the super-resolution (SR) algorithms is to break this boundary, thereby obtaining an image of higher quality with the same physical setup.

There has always been a great demand for producing images with better and better resolution, either by creating a better physical setup, or using post-processing techniques, whether it is about security cameras [33–35], satellites [36–41], professional photography [33, 42–44] or even the HUBBLE space telescope [45–48]. The same rules apply for medical purposes: the higher the resolution of an image, the more precise the diagnosis.

Concerning software-based methods for enhancing image resolution, the algorithm can be used either on sub-pixel-shifted frames by stacking them, or as a post-processing step where even one frame can be satisfactory. The use of SR techniques provides the possibility of receiving a more detailed image at a lower cost compared to the expensive and time-consuming process of building a new hardware capable of delivering the same quality.

Nevertheless, along with other imaging modalities (such as MR, CT or light microscopy) its resolution is heavily dependent on the wavelength (higher frequency,

thus shorter wavelength leads to better resolution), which in the case of sound is a lot poorer than that of light or X-ray. The transducer and its frequency also determine the penetration depth (the higher the frequency, the smaller the mentioned depth is) [49, p. 116]. To be able to examine deeper layers of the medium, lower frequencies should be used, which, however, decreases the resolution.

Taking into account the benefits of US imaging it would be worthwhile if the image resolution and signal-to-noise quality could be improved by post-processing methods. The current doctoral work aims to introduce further scientific knowledge by an experimental method to assess the accuracy of a shift-invariant convolution-based ultrasound image formation model, as well as improving the resolution of ultrasound images.

# New scientific results

**Thesis I:** *I have created an experimental method to assess the accuracy of a shift-invariant convolution-based ultrasound image formation model. The method relies on a planar arrangement of micrometer-scale scatterers in the imaging plane of a linear array. Using the coefficient of determination  $R^2$  to estimate image similarity, the agreement between simulated and real images was  $R^2 = 0.43$  for the RF image and  $R^2 = 0.65$  for the envelope-detected B-mode image.*

Corresponding publication: [Th1]

Models of ultrasound image formation describe the forward process of how an ultrasound image is formed from an acoustic medium. Such models can be used to generate simulated ultrasound images or to obtain quantitative descriptors of the medium from real ultrasound images. A relatively simple and widely used model of image formation treats the ultrasound image (before envelope detection and compression) as the shift-invariant convolution of the imaging system point spread function (PSF) with the scattering function (SF) of the medium [50, 51].

Therefore, I created an experimental method to assess the accuracy of the convolution model. Simulated and real US images were compared to each other. The coefficient of determination was calculated both for the RF ultrasound images and the envelope-detected (B-mode) images.

Various estimates of SF, PSF were tested to see which

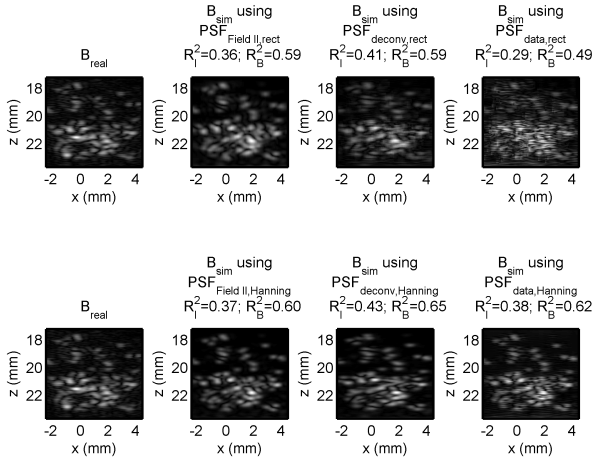


Figure 1: Comparison between the real ultrasound image (first column) and simulated ultrasound images computed using six different estimates of the PSF. It can be observed that using Hanning windowing on the PSF suppresses the high-frequency components and noise at the edges, resulting in better simulation results.  $R_1^2$  stands for the coefficient of determination between the real and simulated RF images, while  $R_B^2$  describes the same for the B-mode images.

yielded the best simulation result. The source of simulation error was also explored, which possibly originates from scattering of the polystyrene particles from multiple reflections, or from microbubbles. From the observations, it is expected that by increasing the concentration of imaged scatterers or by more careful experimental design, higher overall values of the coefficient of determination can be obtained.

The results underline that, at least for the experimental setup used in the current work, the shift-invariant

convolution model describes most of the variation in a B-mode image; however, care should be taken to reduce other sources of scattering such as multiple reflections or microbubbles.

**Thesis II:** *I have presented a novel resolution enhancement technique based on frequency-weighted axial filtering for ultrasound images that can function even when the point-spread function is shift-variant. Estimating resolution using the full-width at half maximum of the autocorrelation, the axial-lateral resolution cell was always improved, with area decreases in the range of 22–94%.*

Corresponding publication: [Th2]

Enhancement of image resolution of ultrasound images is key to help clinicians in finding early indicators of pathological lesions among others. However, the degree of improvement greatly depends on accurately estimating the PSF of the system, which in most cases is spatially variant, thus complicating its approximation and subsequent use in deconvolution.

Therefore, I investigated the possibility of using a method for US images, which is unaffected by depth-dependent effects, and it is also capable of improving the resolution both in the lateral and axial directions. Two simulated and two experimental data sets were used. The nominal central frequencies of the single-element transducers were 20 and 35 MHz. Two different deconvolution methods were used: the classical Wiener filter

Table 1: FWHM values of the AC functions in  $\mu\text{m}$  (lateral  $x$  and axial  $z$ ), and area of the resolution cell ( $x \cdot z \cdot \pi$ ) in  $\mu\text{m}^2$ . It can be seen that the axial-lateral resolution cell (estimated as the area of an ellipse) always improved using the RAMP method.

	orig		deconv		RAMP	
	x	z	x	z	x	z
	$x \cdot z \cdot \pi$		$x \cdot z \cdot \pi$		$x \cdot z \cdot \pi$	
sparse	290.0	27.8	399.8	18.0	222.1	18.7
	25327.5		22608.2		13047.9	
dense	280.4	27.2	412.1	18.0	216.4	18.6
	23960.6		23303.7		12645.0	
phantom	736.0	18.7	152.0	9.0	674.0	14.0
	43238.4		4297.7		29644.1	
skin	723.4	111.7	576.0	39.7	521.0	127.1
	253852.6		71839.4		208033.4	

approach and a custom Fourier domain method (RAMP), where the signal energy was boosted with a gradually increasing function at those (higher) frequencies, where the ultrasound transducer has a weaker response. Both of the methods were used along every A-line separately. The observed resolution was quantified as the FWHM of the mean AC curves. The results confirm that frequency-weighted axial filtering can balance the need for axial and lateral resolution improvement based on their relative values with properly set parameters.

**Thesis III:** *I have shown the successful use of deep learning to enhance scanning acoustic microscope image lateral resolution, even with a very limited data set consisting of rat and mouse brain samples (four images in the training set, each smaller than  $1 \text{ mm} \times 1 \text{ mm}$ ). The estimated images can closely approximate the ground truth*

*data, having an average NRMSE of 0.056, and PSNR of 28.4 dB.*

Corresponding publication: [Th3]

Deep learning is more and more popular nowadays, yet there is limited research about its use on US images, and even those are mostly used for segmentation and classification.

Therefore, I investigated 30- $\mu\text{m}$ -thick rat and mouse brain samples with a high-frequency SAM setup (180 and 316 MHz). The initial training set included 4 full size image pairs, which were co-registered. To create a properly sized training set the full-sized C-scan SAM images were split into tiles of  $300\ \mu\text{m} \times 300\ \mu\text{m}$  with a shift of  $20\ \mu\text{m}$  in-between them. Data augmentation was used to increase the variability and number of samples. A U-Net inspired neural network was used to estimate the high-resolution image based on the low-resolution image, and the 316-MHz data was used as ground truth for quantitative evaluation. Despite the training set being very limited, the results confirm the feasibility of using DL as a single-image SR method to enhance the lateral resolution of SAM images, which greatly outperformed two classical deconvolution methods (Total Variation [TV] and Wiener deconvolution).

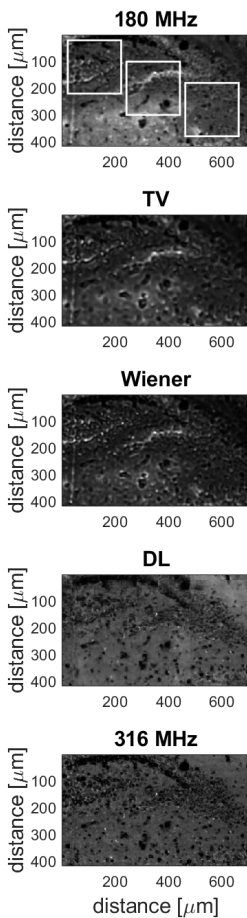
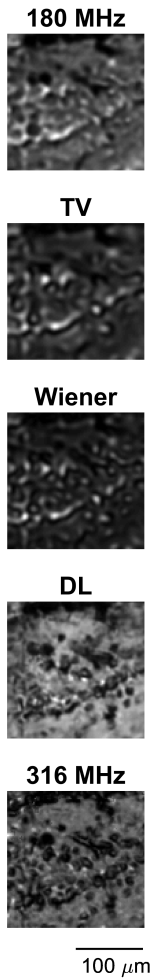
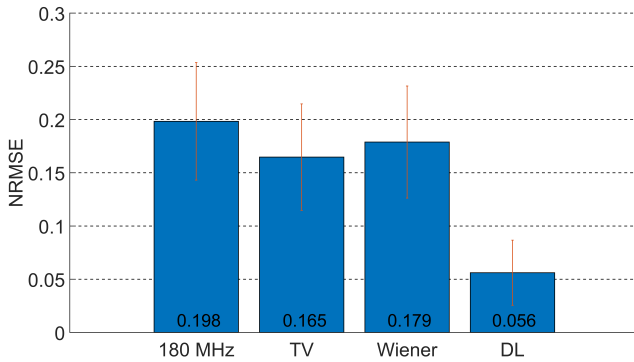


Figure 2: Results of the different resolution enhancement methods on the test image. The images show a rat brain coronal section (Bregma -3.12, the dentate gyrus). From top to bottom: the original 180-MHz image, slice-by-slice TV and Wiener deconvolution methods, DL and the ground truth (316 MHz) image. The top left area indicated by white borders is shown in greater detail in Fig. 3. The DL image was reconstructed from the tiles, therefore, stitching artefacts are present.



*Figure 3: Representative sample from Fig. 2 (top left marked area), showing the hilus. The DL method is seen to qualitatively outperform the classical deconvolution methods in approximating the high-resolution (316 MHz) reference image.*



*Figure 4: NRMSE values of the different image resolution enhancement methods (the red vertical lines showing  $\pm 1$  standard deviation). The images from the resolution enhancement methods were compared to the ground truth data (316 MHz). The values indicate an average considering all of the tiles. The DL method outperformed both the original 180-MHz image and the deconvolution methods. The TV and Wiener deconvolution methods show similar performance to each other, with a slight improvement over the original 180-MHz image.*

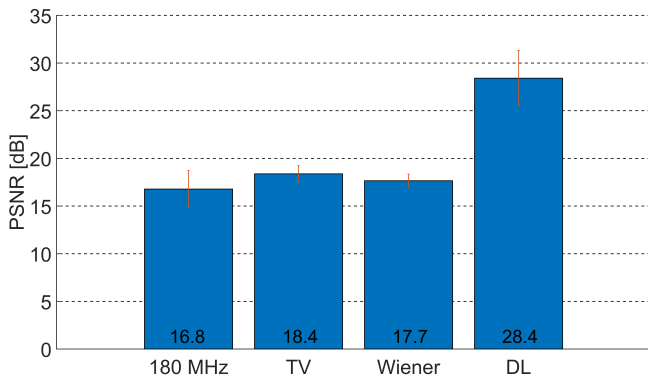


Figure 5: PSNR values of the different image resolution enhancement methods (the red vertical lines showing  $\pm 1$  standard deviation). The images from the resolution enhancement methods were compared to the ground truth data (316 MHz). The values indicate an average considering all of the tiles. The DL method outperformed both the original 180-MHz image and the deconvolution methods. The TV and Wiener deconvolution methods show similar performance to each other, with a slight improvement over the original 180-MHz image.

# Publications related to the thesis

- [Th1] M. Gyöngy and Á. Makra, “Experimental validation of a convolution-based ultrasound image formation model using a planar arrangement of micrometer-scale scatterers,” *IEEE Transactions on Ultrasonics, Ferroelectrics, and Frequency Control*, vol. 62, no. 6, pp. 1211–1219, 2015.
- [Th2] Á. Makra, G. Csány, K. Szalai, and M. Gyöngy, “Simultaneous enhancement of B-mode axial and lateral resolution using axial deconvolution,” *Proceedings of Meetings on Acoustics*, vol. 32, no. 1, 2018.
- [Th3] Á. Makra, W. Bost, I. Kalló, A. Horváth, M. Fournelle, and M. Gyöngy, “Enhancement of acoustic microscopy lateral resolution: A comparison between deep learning and two deconvolution methods,” *IEEE Transactions on Ultrasonics, Ferroelectrics, and Frequency Control*, vol. 67, no. 1, pp. 136–145, 2020.

## Other publications of the author

- [Au1] Á. Makra, “Experimental validation of an ultrasound image formation model,” Bachelor’s Thesis, Pázmány Péter Catholic University, Faculty of Information Technology and Bionics, 2013.
- [Au2] Á. Makra, “An overview of sparsity-based super-resolution algorithms for medical images,” in *PhD Proceedings Annual Issues of the Doctoral School Faculty of Information Technology and Bionics 11*, G. Prószéky and P. Szolgay, Eds. Budapest, Hungary: Pázmány University ePress, 2016, pp. 161 – 164.
- [Au3] Á. Makra, “Design of a rapid scanning acoustic microscope platform for super-resolution research,” in *PhD Proceedings Annual Issues of the Doctoral School Faculty of Information Technology and Bionics 11*, G. Prószéky and P. Szolgay, Eds. Budapest, Hungary: Pázmány University ePress, 2017, pp. 49 – 49.
- [Au4] Á. Makra, “Scanning acoustic microscope system for examining biological tissue,” Master’s Thesis, Pázmány Péter Catholic University, Faculty of Information Technology and Bionics, 2015.
- [Au5] Á. Makra, J. Hatvani, and M. Gyöngy., “Calculation of equivalent ultrasound scatterers using a

time-domain method,” *Jedlik Laboratories Reports*, vol. 3, no. JLR/3-2015, pp. 7 – 12, 2015.

- [Au6] K. Füzési, Á. Makra, and M. Gyöngy, “A stippling algorithm to generate equivalent point scatterer distributions from ultrasound images,” in *Proceedings of Meetings on Acoustics 6ICU*, vol. 32, no. 1. ASA, 2017, p. 020008.

# References

- [1] N. S. Berko, J. N. Le, B. A. Thornhill, D. Wang, A. Negassa, E. S. Amis, and M. Koenigsberg, “Design and validation of a peer-teacher-based musculoskeletal ultrasound curriculum,” *Academic Radiology*, vol. 26, no. 5, pp. 701–706, 2019.
- [2] J. A. Hides, D. H. Cooper, and M. J. Stokes, “Diagnostic ultrasound imaging for measurement of the lumbar multifidus muscle in normal young adults,” *Physiotherapy Theory and Practice*, vol. 8, no. 1, pp. 19–26, 1992.
- [3] R. Coelho, H. Ribeiro, and G. Maconi, “Bowel thickening in crohn’s disease,” *Inflammatory Bowel Diseases*, vol. 23, no. 1, pp. 23–34, 2017.
- [4] G. T. Haar, “Ultrasound focal beam surgery,” *Ultrasound in Medicine & Biology*, vol. 21, no. 9, pp. 1089 – 1100, 1995.
- [5] F. Sammartino, D. W. Beam, J. Snell, and V. Krishna, “Kranion, an open-source environment for planning transcranial focused ultrasound surgery: technical note,” *Journal of Neurosurgery*, pp. 1–7, 2019.
- [6] W. She, T. Cheung, C. R. Jenkins, and M. G. Irwin, “Clinical applications of high-intensity focused ultrasound,” *Hong Kong Medical Journal*, vol. 22, no. 4, pp. 382 – 392, 2016.
- [7] A. Iula, “Ultrasound systems for biometric recognition,” *Sensors*, vol. 19, no. 10, p. 2317, 2019.

- [8] M. Kersemans, E. Verboven, J. Segers, S. Hedaya-trasa, and W. V. Paepegem, “Non-destructive testing of composites by ultrasound, local defect resonance and thermography,” in *Multidisciplinary Digital Publishing Institute Proceedings*, vol. 2, no. 8, 2018, p. 554.
- [9] Z. Remili, Y. Ousten, B. Levrier, E. Suhir, and L. Bechou, “Scanning acoustic microscopy and shear wave imaging mode performances,” *IEEE 65th Electronic Components and Technology Conference (ECTC)*, pp. 2090–2101, 26-29 May 2015.
- [10] A. Phommahaxay, I. D. Wolf, T. Duric, P. Hof-frogge, S. Brand, P. Czurratis, H. Philipsen, G. Beyer, H. Struyf, and E. Beyne, “Defect detection in through silicon vias by GHz scanning acoustic microscopy: key ultrasonic characteristics,” *IEEE 64th Electronic Components and Technology Conference (ECTC)*, pp. 850–855, 27-30 May 2014.
- [11] M. Fan, L. Su, L. Li, W. Wei, Z. He, C. Wong, and X. Lu, “A fuzzy SVM for intelligent diagnosis of solder bumps using scanning acoustic microscopy,” *Semiconductor Technology International Conference (CSTIC)*, 13-14 March 2016.
- [12] F. Naumann and S. Brand, “Numerical prototyping and defect evaluation of scanning acoustic microscopy for advanced failure diagnostics,” *17th International Conference on Thermal, Mechanical and*

*Multi-Physics Simulation and Experiments in Microelectronics and Microsystems*, pp. 1–7, 18–20 April 2016.

- [13] S. Brand, F. Naumann, S. Tismer, B. Boettge, J. Rudzki, F. Osterwald, and M. Petzold, “Non-destructive assessment of reliability and quality related properties of power electronic devices for the in-line application of scanning acoustic microscopy,” *9th International Conference on Integrated Power Electronics Systems (CIPS)*, 8–10 March 2016.
- [14] S. Brand, E. C. Weiss, R. M. Lemor, and M. C. Kolios, “High frequency ultrasound tissue characterization and acoustic microscopy of intracellular changes,” *Ultrasound in Medicine and Biology*, vol. 34, pp. 1396–1407, 2008.
- [15] E. Grünwald, R. Hammer, R. Jördis, B. Sartory, and R. Brunner, “Accretion detection via scanning acoustic microscopy in microelectronic components—considering symmetry breaking effects,” *Microscopy and Microanalysis 23*, vol. 23, pp. 1466–1467, 2017.
- [16] M. Kim, N. Choi, Y. I. Kim, and Y. H. Lee, “Characterization of RF sputtered zinc oxide thin films on silicon using scanning acoustic microscopy,” *Journal of Electroceramics*, pp. 1–9, 2017.
- [17] D. Wang, X. He, Z. Xu, W. Jiao, F. Yang, L. Jiang, L. Li, W. Liu, and R. Wang, “Study on damage evalu-

ation and machinability of UD-CFRP for the orthogonal cutting operation using scanning acoustic microscopy and the finite element method,” *Materials*, vol. 10, p. 204, 2017.

- [18] J. Dong, X. Wu, A. Locquet, and D. S. Citrin, “Terahertz superresolution stratigraphic characterization of multilayered structures using sparse deconvolution,” *IEEE TRANSACTIONS ON TERAHERTZ SCIENCE AND TECHNOLOGY*, vol. 7, pp. 260–267, 2017.
- [19] M. S. Firouz, A. Farahmandi, and S. Hosseinpour, “Recent advances in ultrasound application as a novel technique in analysis, processing and quality control of fruits, juices and dairy products industries: A review,” *Ultrasonics Sonochemistry*, vol. 57, pp. 73–88, 2019.
- [20] N. Segura, M. Amarillo, N. Martinez, M. Grompone *et al.*, “Improvement in the extraction of hass avocado virgin oil by ultrasound application,” *J. Food Res*, vol. 7, pp. 106–113, 2018.
- [21] J. M. del Fresno, I. Loira, A. Morata, C. González, J. A. Suárez-Lepe, and R. Cuerda, “Application of ultrasound to improve lees ageing processes in red wines,” *Food Chemistry*, vol. 261, pp. 157–163, 2018.
- [22] V. Akdeniz and A. S. Akalın, “New approach for yoghurt and ice cream production: High-intensity ultra-

sound,” *Trends in Food Science & Technology*, vol. 86, pp. 392 – 398, 2019.

- [23] D. Rohrbach, B. Wodlinger, J. Wen, J. Mamou, and E. Feleppa, “High-frequency quantitative ultrasound for imaging prostate cancer using a novel micro-ultrasound scanner,” *Ultrasound in Medicine & Biology*, vol. 44, no. 7, pp. 1341–1354, 2018.
- [24] T. Mizoguchi, K. Tamura, J. Mamou, J. A. Ketterling, K. Yoshida, and T. Yamaguchi, “Comprehensive backscattering characteristics analysis for quantitative ultrasound with an annular array: a basic study on homogeneous scattering phantom,” *Japanese Journal of Applied Physics*, vol. 58, no. SG, p. SGGE08, 2019.
- [25] M. L. Oelze and J. Mamou, “Review of quantitative ultrasound: Envelope statistics and backscatter coefficient imaging and contributions to diagnostic ultrasound,” *IEEE Transactions on Ultrasonics, Ferroelectrics, and Frequency Control*, vol. 63, no. 2, pp. 336 – 351, 2016.
- [26] E. J. Feleppa, J. Mamou, and D. Rohrbach, “Typing and imaging of biological and non-biological materials using quantitative ultrasound,” 2019, uS Patent 10,338,033.
- [27] J. Mamou, P. Goundan, D. Rohrbach, H. Patel, E. Feleppa, and S. Lee, “In-vivo-quantitative-ultrasound assessment of thyroid nodules,” *The Jour-*

*nal of the Acoustical Society of America*, vol. 146, no. 4, pp. 2811 – 2812, 2019.

- [28] S. C. Lin, E. Heba, T. Wolfson, B. Ang, A. Gamst, A. Han, J. W. Erdman, W. D. O’Brien, M. P. Andre, C. B. Sirlin, and R. Loomba, “Noninvasive diagnosis of nonalcoholic fatty liver disease and quantification of liver fat using a new quantitative ultrasound technique,” *Clinical Gastroenterology and Hepatology*, vol. 13, no. 7, pp. 1337–1345.e6, 2015.
- [29] L. C. Slane, J. Martin, R. DeWall, D. Thelen, and K. Lee, “Quantitative ultrasound mapping of regional variations in shear wave speeds of the aging achilles tendon,” *European Radiology*, vol. 27, no. 2, pp. 474–482, 2016.
- [30] N. G. Simon, J. W. Ralph, C. Lomen-Hoerth, A. N. Poncelet, S. Vucic, M. C. Kiernan, and M. Kliot, “Quantitative ultrasound of denervated hand muscles,” *Muscle & Nerve*, vol. 52, no. 2, pp. 221–230, 2015.
- [31] J. S. Paige, G. S. Bernstein, E. Heba, E. A. Costa, M. Ferreira, T. Wolfson, A. C. Gamst, M. A. Valasek, G. Y. Lin, A. Han *et al.*, “A pilot comparative study of quantitative ultrasound, conventional ultrasound, and mri for predicting histology-determined steatosis grade in adult nonalcoholic fatty liver disease,” *American Journal of Roentgenology*, vol. 208, no. 5, pp. W168–W177, 2017.

- [32] J. Mamou, D. Rohrbach, E. Saegusa-Beecroft, E. Yanagihara, J. Machi, and E. J. Feleppa, “Ultrasound-scattering models based on quantitative acoustic microscopy of fresh samples and unstained fixed sections from cancerous human lymph nodes,” in *2015 IEEE International Ultrasonics Symposium (IUS)*. IEEE, 2015.
- [33] P. Howell, “Resolution-enhancement method for digital imaging,” 2003, uS Patent 6,570,613.
- [34] A. Kumar, S. G. Eranirose, and A. K. Lakshmikumar, “Multi-resolution ip camera,” 2013, uS Patent App. 13/447,202.
- [35] V. A. Trofimov and V. V. Trofimov, “IR camera temperature resolution enhancing using computer processing of IR image,” in *Thermosense: Thermal Infrared Applications XXXVIII*, J. N. Zalameda and P. Bison, Eds. SPIE, 2016.
- [36] H. Demirel and G. Anbarjafari, “Satellite image resolution enhancement using complex wavelet transform,” *IEEE Geoscience and Remote Sensing Letters*, vol. 7, no. 1, pp. 123–126, 2010.
- [37] O. Harikrishna and A. Maheshwari, “Satellite image resolution enhancement using dwt technique,” *International Journal of Soft Computing and Engineering (IJSCE)*, vol. 2, no. 5, pp. 274 – 278, 2012.

- [38] H. Demirel and G. Anbarjafari, “Discrete wavelet transform-based satellite image resolution enhancement,” *IEEE Transactions on Geoscience and Remote Sensing*, vol. 49, no. 6, pp. 1997–2004, 2011.
- [39] M. Z. Iqbal, A. Ghafoor, and A. M. Siddiqui, “Satellite image resolution enhancement using dual-tree complex wavelet transform and nonlocal means,” *IEEE Geoscience and Remote Sensing Letters*, vol. 10, no. 3, pp. 451–455, 2013.
- [40] P. Rasti, I. Lusi, H. Demirel, R. Kiefer, and G. Anbarjafari, “Wavelet transform based new interpolation technique for satellite image resolution enhancement,” in *2014 IEEE International Conference on Aerospace Electronics and Remote Sensing Technology*. IEEE.
- [41] M. Farrar and E. Smith, “Spatial resolution enhancement of terrestrial features using deconvolved SSM/i microwave brightness temperatures,” *IEEE Transactions on Geoscience and Remote Sensing*, vol. 30, no. 2, pp. 349–355, 1992.
- [42] G. Daniell and S. Gull, “Maximum entropy algorithm applied to image enhancement,” *IEE Proceedings E-Computers and Digital Techniques*, vol. 127, no. 5, pp. 170–172, 1980.
- [43] E. Eisemann and F. Durand, “Flash photography enhancement via intrinsic relighting,” in *ACM transac-*

- tions on graphics (TOG)*, vol. 23, no. 3. ACM, 2004, pp. 673–678.
- [44] T. Mertens, J. Kautz, and F. V. Reeth, “Exposure fusion: A simple and practical alternative to high dynamic range photography,” *Computer Graphics Forum*, vol. 28, no. 1, pp. 161–171, 2009.
- [45] T. Schulz, B. Stribling, and J. Miller, “Multiframe blind deconvolution with real data: imagery of the hubble space telescope,” *Optics Express*, vol. 1, no. 11, p. 355, 1997.
- [46] A. S. Carasso, “APEX blind deconvolution of color hubble space telescope imagery and other astronomical data,” *Optical Engineering*, vol. 45, no. 10, p. 107004, 2006.
- [47] J. L. Hershey, “A deconvolution technique for hubble space telescope fgs fringe analysis,” *Publications of the Astronomical Society of the Pacific*, vol. 104, no. 677, pp. 592 – 596, 1992.
- [48] R. L. White, “Image restoration using the damped lucy–richardson method,” in *Instrumentation in Astronomy VIII*, D. L. Crawford and E. R. Craine, Eds. SPIE, 1994.
- [49] T. L. Szabo, *Diagnostic Ultrasound Imaging: Inside Out*. Academic Press, 2004.

- [50] J. C. Bamber and R. Dickinson, “Ultrasonic B-scanning: A computer simulation,” *Phys. Med. Biol.*, vol. 25, no. 3, pp. 463–479, 1980.
- [51] C. R. Hill, J. C. Bamber, and G. R. ter Haar, *Physical Principles of Medical Ultrasonics*, 2nd ed. Chichester, UK:John Wiley and Sons, 2004.

